

# In silico Approach to Identify Novel Thiazolidin-4-ones Against *Staphylococcus aureus*

Rajala Srikala<sup>1</sup>, S. Mohanalakshmi<sup>2</sup>

<sup>1</sup>Research Scholar, Jawaharlal Nehru Technological University Anantapur, Anantapur, Andhra Pradesh, India,

<sup>2</sup>Director, Amity Institute of Pharmacy, Amity University, Gwalior, Madhya Pradesh, India

## Abstract

**Introduction:** The DHFR inhibitors perform a significant role in thymidine synthesis by blocking the DHFR and interference with this pathway inhibits bacterial DNA synthesis. In this article, a molecular docking study followed by in silico pharmacokinetic parameters could be studied as an effective approach to detect newer DHFR inhibitors. **Methods:** Novel Thiazolidin-4-one derivatives were designed to perform molecular docking studies using Autodock-1.5.6 and identified the hit molecules. The hits were further evaluated for their drug likeliness using the Swiss ADME web server. **Results:** The binding affinity of the designed ligands towards DHFR was selected based on binding affinities and interaction patterns. Almost all the compounds have good binding affinities in the range of -10.4 to -5.6 and -11.0 to -8.0 compared with that of cognate ligand -7.6 and -7.9 for wild and mutant DHFR, respectively. **Conclusion:** The results reveal that Thiazolidin-4-ones as DHFR inhibitors and among 56 compounds, except 5 compounds all compounds showing good binding affinities may produce significant anti-staphylococcal activity for further enhancement.

**Key words:** Autodock, DHFR inhibitors, discovery studio, *in silico*, Swiss ADME

## INTRODUCTION

Infectious diseases are a significant threat worldwide as new microorganism resistance to antibiotics inflates issues concerning the continual utilization of medicament agents in clinical observation. Thus, there is a requirement to develop new medication for the effective treatment of microorganism infections is a major priority. One of the ways enforced to inhibit bacterial pathogens is to target the synthesis pathway of nucleic acids, wherever the DHFR plays a significant role. The aptness of targeting DHFR for combating *Staphylococcus aureus* has been valid by the drug Trimethoprim, a very powerful anti-staphylococcal agent.<sup>[1-3]</sup> Supported many ligand- or structure-based approaches, varied categories of inhibitors are investigated, as alkali analogs.<sup>[4-6]</sup> However, only a few of them inhibit *in vitro* growth of microorganisms.

There is a requirement to develop new chemical entities to inhibit the DHFR catalyst. Thiazolidin-4-one is taken into account as a biologically active scaffold that possesses the majority sorts of biological activities. Thiazolidin-4-ones are with success introduced in numerous classes

and evidenced as potential moieties, like thiazolidomycin activity against *Streptomyces* species, Ralitolone as a potent antiepileptic, Pioglitazone as a hypoglycemic agent, Etozolin as an antihypertensive agent. This variation within the biological response profile has engrossed the eye of many researchers to find this skeleton to its various potentials against many activities.<sup>[7]</sup> Kerru *et al.*, Patel *et al.*, Mandal *et al.*, Saini *et al.*, Ghoneim and Zordok, and several other additional researchers have connected Thiazolidin-4-ones as antimicrobial agents.<sup>[8-12]</sup> With sure variations, these compounds may generate potent chemical entities against *Staphylococci* species.

In this regard, within the current study, we tend to have designed various sets of novel thiazolidin-4-ones bearing aryl and diaryl substitutions at C2 and N3 positions, unsubstituted and alkyl radical substitution at the C5 position and performed *in silico* analysis of the designed moieties.<sup>[13]</sup>

### Address for correspondence:

Rajala Srikala,  
Jawaharlal Nehru Technological University  
Anantapur, Anantapur, Andhra Pradesh, India.  
E-mail: srikala.rajala@gmail.com

**Received:** 28-05-2022

**Revised:** 13-09-2022

**Accepted:** 01-10-2022

**Table 1: Structures of designed compounds (1-56)**

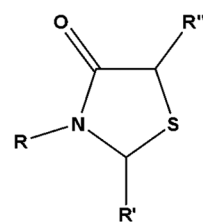
Code	R	R'	R''
01	2M2MBP	4,5,6-trimethylpyrimidin-2-yl	H
02	2M2MBP	4,5,6-trimethylpyrimidin-2-yl	CH <sub>3</sub>
03	2M2MBP	4-hydroxy-5-methylpyrimidin-2-yl	H
04	2M2MBP	4-hydroxy-5-methylpyrimidin-2-yl	CH <sub>3</sub>
05	2M2MBP	pyrimidin-2-yl	H
06	2M2MBP	pyrimidin-2-yl	CH <sub>3</sub>
07	2M2MBP	4-chloropyrimidin-2-yl	H
08	2M2MBP	4-chloropyrimidin-2-yl	CH <sub>3</sub>
09	2M2MBP	2-chloropyrimidin-4-yl	H
10	2M2MBP	2-chloropyrimidin-4-yl	CH <sub>3</sub>
11	2M2MBP	pyrimidin-5-yl	H
12	2M2MBP	pyrimidin-5-yl	CH <sub>3</sub>
13	2M2MBP	2-chloropyrimidin-5-yl	H
14	2M2MBP	2-chloropyrimidin-5-yl	CH <sub>3</sub>
15	5M2MBP	4-chloropyrimidin-2-yl	CH <sub>3</sub>
16	5M2MBP	2-chloropyrimidin-5-yl	CH <sub>3</sub>
17	5M2MBP	4-hydroxy-5-methylpyrimidin-2-yl	H
18	5M2MBP	4-chloropyrimidin-2-yl	H
19	5M2MBP	2-chloropyrimidin-5-yl	H
20	5M2MBP	2-chloropyrimidin-4-yl	CH <sub>3</sub>
21	5M2MBP	pyrimidin-2-yl	CH <sub>3</sub>
22	5M2MBP	pyrimidin-5-yl	CH <sub>3</sub>
23	5M2MBP	2-chloropyrimidin-4-yl	H
24	5M2MBP	pyrimidin-5-yl	H
25	5M2MBP	4,5,6-trimethylpyrimidin-2-yl	H
26	5M2MBP	pyrimidin-2-yl	H
27	5M2MBP	4-hydroxy-5-methylpyrimidin-2-yl	CH <sub>3</sub>
28	5M2MBP	4,5,6-trimethylpyrimidin-2-yl	CH <sub>3</sub>
29	5M3MBP	4-chloropyrimidin-2-yl	CH <sub>3</sub>
30	5M3MBP	pyrimidin-2-yl	H
31	5M3MBP	2-chloropyrimidin-5-yl	H
32	5M3MBP	4-hydroxy-5-methylpyrimidin-2-yl	H
33	5M3MBP	4,5,6-trimethylpyrimidin-2-yl	H
34	5M3MBP	4-chloropyrimidin-2-yl	H
35	5M3MBP	pyrimidin-5-yl	H
36	5M3MBP	2-chloropyrimidin-5-yl	CH <sub>3</sub>
37	5M3MBP	pyrimidin-2-yl	CH <sub>3</sub>
38	5M3MBP	2-chloropyrimidin-4-yl	H
39	5M3MBP	pyrimidin-5-yl	CH <sub>3</sub>
40	5M3MBP	2-chloropyrimidin-4-yl	CH <sub>3</sub>
41	5M3MBP	4-hydroxy-5-methylpyrimidin-2-yl	CH <sub>3</sub>
42	5M3MBP	4,5,6-trimethylpyrimidin-2-yl	CH <sub>3</sub>
43	5M4MBP	2-chloropyrimidin-5-yl	H
44	5M4MBP	pyrimidin-2-yl	H

(Contd...)

**Table 1: (Continued)**

Code	R	R'	R''
45	5M4MBP	2-chloropyrimidin-5-yl	CH <sub>3</sub>
46	5M4MBP	4-hydroxy-5-methylpyrimidin-2-yl	H
47	5M4MBP	4-chloropyrimidin-2-yl	H
48	5M4MBP	4-chloropyrimidin-2-yl	CH <sub>3</sub>
49	5M4MBP	2-chloropyrimidin-4-yl	H
50	5M4MBP	pyrimidin-5-yl	H
51	5M4MBP	pyrimidin-5-yl	CH <sub>3</sub>
52	5M4MBP	4-hydroxy-5-methylpyrimidin-2-yl	CH <sub>3</sub>
53	5M4MBP	4,5,6-trimethylpyrimidin-2-yl	H
54	5M4MBP	2-chloropyrimidin-4-yl	CH <sub>3</sub>
55	5M4MBP	pyrimidin-2-yl	CH <sub>3</sub>
56	5M4MBP	4,5,6-trimethylpyrimidin-2-yl	CH <sub>3</sub>

2M2MBP - 2-methoxy-2'-methyl-[1,1'-biphenyl]-4-yl;  
 5M2MBP - 5-methoxy-2'-methyl-[1,1'-biphenyl]-3-yl;  
 5M3MBP - 5-methoxy-3'-methyl-[1,1'-biphenyl]-3-yl;  
 5M4MBP - 5-methoxy-4'-methyl-[1,1'-biphenyl]-3-yl

**Figure 1: General structure of thiazolidin-4-one**

## MATERIALS AND METHODS

### Molecular docking

Chemical structures of unique thiazolidin-4-one derivatives were proposed using literature. Flexible-ligand docking simulations were executed with AutoDock version 1.5.6. X-ray crystallographic structure of DHFR enzyme was taken from the protein data bank (2W9H and 5ISQ;<sup>[14,15]</sup> <http://www.rcsb.org/>) with resolution 1.48 Å and 1.90 Å.

For the preparation of a target protein, crystallographic ligand (Trimethoprim and 3'-(3-(2,4-diamino-6-ethylpyrimidin-5-yl)propan-1-yl)-4'-methoxy-[1,1'-biphenyl]-4-carboxylic acid (UCP1106)), NAP, EDO, and water molecules were all removed from the original structure. All the pre-processing steps for DHFR protein were executed through AutoDock Tools 1.5.6 program (ADT).<sup>[16]</sup> ADT program was operated to fuse the non-polar hydrogens into the associated carbon atoms of the receptor and Kollman charges were allocated.

Ligands were designed using ChemSketch ([www.acdlabs.com](http://www.acdlabs.com)) [Figure 1 and Table 1], and the file formats are converted from .mol to .pdb format using Open Babel.<sup>[17]</sup> Then

**Table 2:** Binding energies and interacted amino acids for compounds 1-56 with DHFR (2W9H and 5ISQ)

Code	Wild DHFR Binding affinity	Mutant DHFR Binding affinity
Reference	-7.6	-7.9
1	-6.5	-8
2	-5.6	-8.4
3	-9.2	-8.3
4	-8.6	-8.5
5	-8.2	-8.4
6	-8.4	-8.7
7	-8.4	-9
8	-8.6	-9.3
9	-8.1	-9.9
10	-8.6	-8.5
11	-7.9	-9.4
12	-8	-9.4
13	-8.1	-9.2
14	-7.5	-9.4
15	-9.5	-10.6
16	-9.3	-10.5
17	-9.5	-9.9
18	-9.2	-10.2
19	-9	-10.3
20	-9.4	-9.8
21	-9.1	-10.1
22	-8.8	-10.2
23	-8.7	-10.2
24	-8.3	-10.6
25	-9.1	-9.5
26	-8.8	-9.8
27	-8.5	-9.1
28	-7.4	-8.5
29	-10.4	-10.9
30	-10.3	-10.2
31	-10	-10.3
32	-9.9	-10.2
33	-9.6	-10.3
34	-9.5	-10.1
35	-9.3	-10.3
36	-9.3	-10.3
37	-8.6	-10.6
38	-8.5	-10.4
39	-8.7	-10.1
40	-8.9	-9.6
41	-8.6	-9.6

(Contd...)

**Table 2: (Continued)**

Code	Wild DHFR Binding affinity	Mutant DHFR Binding affinity
42	-7.3	-9.4
43	-9.9	-10.8
44	-10.2	-10.1
45	-9.4	-10.6
46	-9.7	-10.2
47	-9.7	-10.1
48	-10.2	-9.5
49	-8.7	-10.7
50	-8.4	-11
51	-8.8	-10.4
52	-9.2	-10
53	-8.8	-10
54	-8.9	-9.8
55	-9.5	-9.2
56	-8	-8.9

non-polar hydrogens, Gasteiger charges, and torsion degrees of freedom were assigned by the ADT program. Lamarckian genetic algorithm (LGA) employed to model the interactions between thiazolidin-4-ones and DHFR active site using 100 GA runs; 27000 maximum generations; a gene mutation rate of 0.02; and a crossover rate of 0.8 were operated for LGA method. Based on the validation study, the cognate (co-crystallographic) ligand was extracted and re-docked into its receptor (self-docking). Validation is performed by comparing the root mean square deviation of the Cartesian coordinates of the atoms of the ligand in the docked pose and crystallographic conformations.

DHFR was characterized by grid maps in the actual docking procedure. The grids were calculated using the AutoGrid module. The grid included a map for every atom type within the ligand and also a map for electrostatic interactions. The size of the grid was  $50 \times 50 \times 50 \text{ \AA}$  (distributed in the x, y, and z directions) and it was centered on the center of mass of the catalytic site of DHFR with a spacing of  $0.375 \text{ \AA}$ . Cluster analysis was performed on the docked results concerning RMS tolerance of  $2 \text{ \AA}$ . 2D and 3D interactions of the docked ligands were analyzed using Discovery Studio Visualizer-20.1 (<https://discover.3ds.com/discovery-studio-visualizer-download>).

### ***In silico* pharmacokinetic parameters**

The *in silico* drug likeliness and ADME properties of the proposed molecules were determined by using the SwissADME webserver.<sup>[18-20]</sup> In this server, the structure was drawn or the SMILES format of the ligands was incorporated and executed the program to attain the desired results.

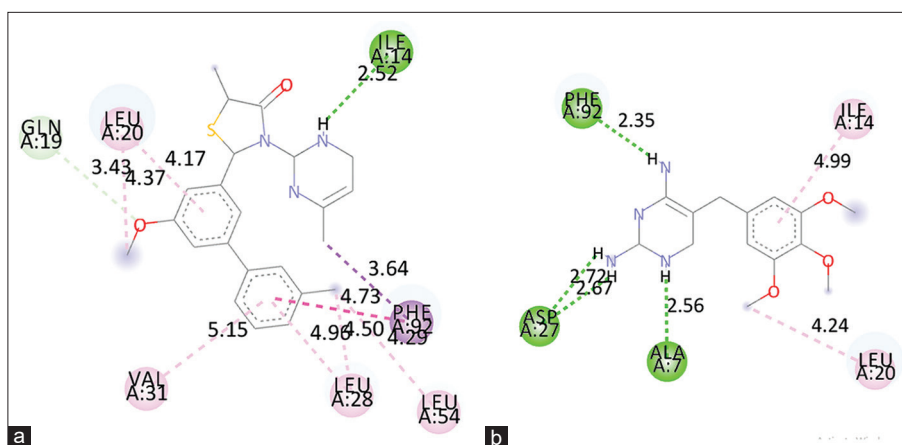


**Figure 2:** 2D interactions of Cognate ligand with active site of DHFR (a) 2W9H and (b) 5ISQ. Green – H-bond interaction, Rose – Alkyl/Pi-Alkyl interactions, Violet – Pi-Sigma interactions

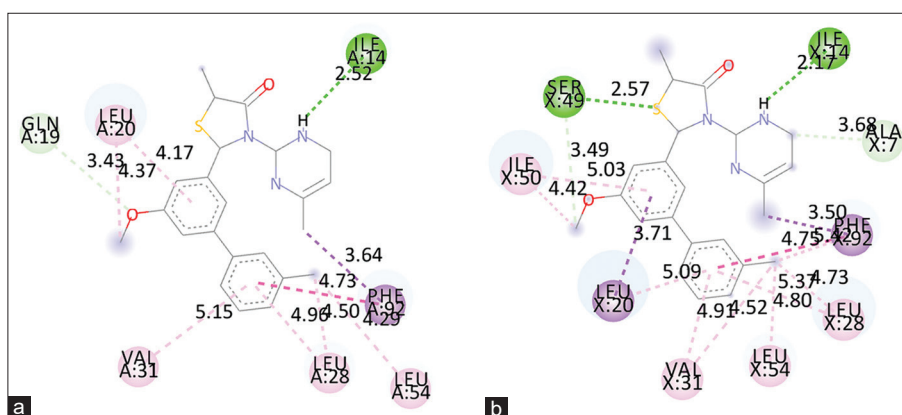


**Figure 3:** 2D interactions of docked compound 29 with DHFR (a) 2W9H and (b) 5ISQ

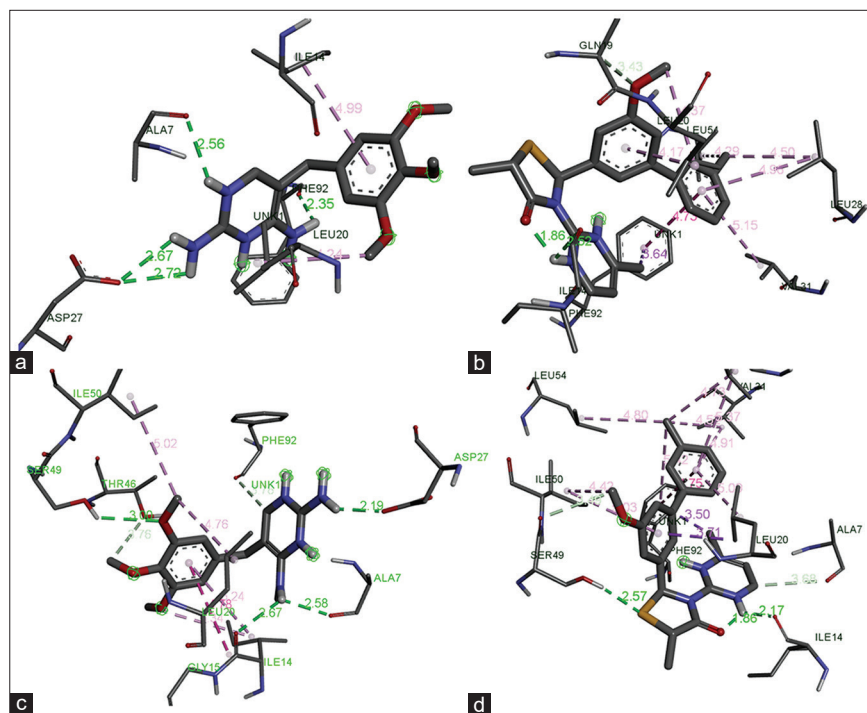


**Figure 4:** 3D structures of best affinity mode of docked compounds (a) Reference with Wild DHFR (b) 29 with Wild DHFR (c) Reference with Mutant DHFR (d) 29 with Mutant DHFR

**Table 3:** Molecular properties for designed compounds 1-56

Code	MW	H-bond donors	H-bond acceptors	Log P	Rotatable bonds	MR	TPSA
Ref	290.32	2	5	2.21	5	79.77	105.51
1	419.54	0	4	3.86	4	125.94	80.62
2	433.57	0	4	4.15	4	130.74	80.62
3	407.49	1	5	3.32	4	118.03	100.85
4	421.51	1	5	3.56	4	122.84	100.85
5	377.46	0	4	3.09	4	111.04	80.62
6	391.49	0	4	3.34	4	115.85	80.62
7	411.9	0	4	3.36	4	116.05	80.62
8	425.93	0	4	3.66	4	120.86	80.62
9	411.9	0	4	3.17	4	116.05	80.62
10	425.93	0	4	3.4	4	120.86	80.62
11	377.46	0	4	3.12	4	111.04	80.62
12	391.49	0	4	3.3	4	115.85	80.62
13	411.9	0	4	3.45	4	116.05	80.62
14	425.93	0	4	3.74	4	120.86	80.62
15	425.93	0	4	3.63	4	120.86	80.62
16	425.93	0	4	3.77	4	120.86	80.62
17	407.49	1	5	3.37	4	118.03	100.85
18	411.9	0	4	3.42	4	116.05	80.62
19	411.9	0	4	3.51	4	116.05	80.62
20	425.93	0	4	3.5	4	120.86	80.62
21	391.49	0	4	3.38	4	115.85	80.62
22	391.49	0	4	3.43	4	115.85	80.62
23	411.9	0	4	3.25	4	116.05	80.62
24	377.46	0	4	3.16	4	111.04	80.62
25	419.54	0	4	3.7	4	125.94	80.62
26	377.46	0	4	3.09	4	111.04	80.62
27	421.51	1	5	3.73	4	122.84	100.85
28	433.57	0	4	4.04	4	130.74	80.62
29	425.93	0	4	3.75	4	120.86	80.62
30	377.46	0	4	3.23	4	111.04	80.62
31	411.9	0	4	3.66	4	116.05	80.62
32	407.49	1	5	3.41	4	118.03	100.85
33	419.54	0	4	3.83	4	125.94	80.62
34	411.9	0	4	3.48	4	116.05	80.62
35	377.46	0	4	3.28	4	111.04	80.62
36	425.93	0	4	3.89	4	120.86	80.62
37	391.49	0	4	3.53	4	115.85	80.62
38	411.9	0	4	3.38	4	116.05	80.62
39	391.49	0	4	3.59	4	115.85	80.62
40	425.93	0	4	3.65	4	120.86	80.62
41	421.51	1	5	3.72	4	122.83	100.85
42	433.57	0	4	4.12	4	130.74	80.62
43	411.9	0	4	3.64	4	116.05	80.62

(Contd...)

Table 3: (Continued)

Code	MW	H-bond donors	H-bond acceptors	Log P	Rotatable bonds	MR	TPSA
44	377.46	0	4	3.23	4	111.04	80.62
45	425.93	0	4	3.87	4	120.86	80.62
46	407.49	1	5	3.38	4	118.03	100.85
47	411.9	0	4	3.53	4	116.05	80.62
48	425.93	0	4	3.82	4	120.86	80.62
49	411.9	0	4	3.34	4	116.05	80.62
50	377.46	0	4	3.25	4	111.04	80.62
51	391.49	0	4	3.53	4	115.85	80.62
52	421.51	1	5	3.8	4	122.83	100.85
53	419.54	0	4	3.79	4	125.94	80.62
54	425.93	0	4	3.66	4	120.86	80.62
55	391.49	0	4	3.53	4	115.85	80.62
56	433.57	0	4	4.11	4	130.74	80.62
Recommended values	<500 Daltons	≤5	≤10	≤5	≤10	40 to 130	≤140 Å <sup>2</sup>

MW: Molecular weight, MR: Molar refractivity, TPSA: Total polar surface area

Table 4: ADME and synthetic accessibility for designed compounds 1-56

Code	Aqueous solubility	P-gp substrate	log Kp (cm/s)	Synthetic accessibility
Reference	Soluble	Yes	-7.42	2.58
1	Moderately soluble	Yes	-5.24	3.98
2	Poorly soluble	Yes	-5.04	4.35
3	Moderately soluble	No	-5.75	3.89
4	Moderately soluble	No	-5.55	4.26
5	Moderately soluble	No	-5.81	3.57
6	Moderately soluble	No	-5.61	3.94
7	Moderately soluble	No	-5.33	3.63
8	Poorly soluble	No	-5.14	4
9	Moderately soluble	No	-5.33	3.64
10	Poorly soluble	No	-5.14	4.03
11	Moderately soluble	Yes	-6.05	3.61
12	Moderately soluble	No	-5.84	3.97
13	Moderately soluble	No	-5.57	3.68
14	Moderately soluble	No	-5.37	4.04
15	Poorly soluble	No	-5.14	4.04
16	Moderately soluble	No	-5.37	4.09
17	Moderately soluble	No	-5.75	3.93
18	Moderately soluble	No	-5.33	3.67
19	Moderately soluble	No	-5.57	3.73
20	Poorly soluble	No	-5.14	4.06
21	Moderately soluble	No	-5.61	3.98
22	Moderately soluble	No	-5.84	4.01
23	Moderately soluble	No	-5.33	3.67
24	Moderately soluble	No	-6.05	3.66

(Contd...)

Table 4: (Continued)

Code	Aqueous solubility	P-gp substrate	log Kp (cm/s)	Synthetic accessibility
25	Moderately soluble	Yes	-5.24	4.02
26	Moderately soluble	No	-5.81	3.62
27	Moderately soluble	No	-5.55	4.29
28	Poorly soluble	Yes	-5.04	4.39
29	Poorly soluble	No	-5.14	4.01
30	Moderately soluble	No	-5.81	3.58
31	Moderately soluble	No	-5.57	3.69
32	Moderately soluble	No	-5.75	3.9
33	Moderately soluble	Yes	-5.24	3.98
34	Moderately soluble	No	-5.33	3.63
35	Moderately soluble	No	-6.05	3.62
36	Moderately soluble	No	-5.37	4.05
37	Moderately soluble	No	-5.61	3.95
38	Moderately soluble	No	-5.33	3.65
39	Moderately soluble	No	-5.84	3.97
40	Poorly soluble	No	-5.14	4.03
41	Moderately soluble	No	-5.55	4.26
42	Poorly soluble	Yes	-5.04	4.35
43	Moderately soluble	No	-5.57	3.7
44	Moderately soluble	No	-5.81	3.6
45	Moderately soluble	No	-5.37	4.06
46	Moderately soluble	No	-5.75	3.91
47	Moderately soluble	No	-5.33	3.65
48	Poorly soluble	No	-5.14	4.02
49	Moderately soluble	No	-5.33	3.66
50	Moderately soluble	No	-6.05	3.63
51	Moderately soluble	No	-5.84	3.99
52	Moderately soluble	No	-5.55	4.28
53	Moderately soluble	Yes	-5.24	3.99
54	Poorly soluble	No	-5.14	4.05
55	Moderately soluble	No	-5.61	3.96
56	Poorly soluble	Yes	-5.04	4.36

log Kp: Skin permeation

## RESULTS AND DISCUSSION

The docking study of designed thiazolidin-4-ones to the active site of protein was performed by Autodock for calculating the binding affinities of the designed ligands with the protein. The designed molecules were docked into the DHFR (2W9H and 5ISQ), to determine their DHFR inhibitory activity. All compounds except 1, 2, 14, 28, and 42 had shown a good binding affinity to both wild and mutant DHFR receptors compared to the cognate ligand for anti-staphylococcal activity [Table 2]. From Table 1, the interactions are mainly due to the lipophilic factors and hydrogen bonding. The interactions with wild and mutant DHFR are mainly

subjugated in the region of ALA7, ILE14, and SER49 residues which are in the active site region [Figure 2]. The aryl substitutions are located in the hydrophobic pocket and the amino group is located in the hydrophilic pocket. The compound 29 exhibited hydrogen bonding with ILE14 (H-bond length 2.52 Å) residue of wild DHFR and hydrogen bonding with ILE14, SER 49 (H-bond length 2.17 Å and 2.57 Å, respectively) residues of mutant DHFR, which is depicted in Figure 3. The best-docked poses of the compounds 29, 30 and 29, 50 for wild and mutant DHFR with significant binding affinities are shown in Figure 4.

The ADMET properties for the thiazolidin-4-ones 1-56 were determined *in silico* using the SwissADME webserver of

the Swiss Institute of Bioinformatics. Molecular weights of the compounds are between 377.46 and 433.57 g.mol<sup>-1</sup>. Estimated no. of hydrogen bond donors are in the range of 0–1, hydrogen bond acceptors are in the range of 4–5. LogP, molar refractivity, rotatable bonds, and total polar surface area of the compounds are between 3.09 and 4.15; 111.04 and 130.74; 4; 80.62 and 100.85 Å<sup>2</sup>, respectively. The compounds are in the range of Lipinski's rule of five and Veber's rule [Table 3].

All the compounds are showing moderate to poor aqueous solubility which indeed results in high gastro-intestinal (GI) absorption. All the compounds are not crossing the blood-brain barrier. Skin permeation values are found in the range of –6.05 to –5.04 cm/s. 01, 02, 11, 25, 28, 33, 42, 53, and 56 are P-gp substrates which can decrease drug accumulation in multidrug-resistant cells. The details of the ADME properties for compounds 1-56 are shown in Table 4.

Besides, synthetic accessibility of the compounds can be predicted using Swiss ADME on a scale of 1-10, that is, very easy to difficult to synthesize. All the designed compounds can be easily synthesized in the laboratory.

Bioavailability of all 1-56 compounds was found to be 0.55.

## CONCLUSION

The docking study revealed that the thiazolidin-4-ones showed better alignment than the new experimental drugs at the active site by interacting with active site amino acid residues of DHFR (2W9H and 5ISQ). Thus, the *in silico* method adopted in the present study helped in identifying the lead molecules to inhibit DHFR. Results observed in the present study demonstrated that some derivatives of the designed thiazolidin-4-ones may exert interesting anti-staphylococcal activity. The compounds 29, 30, and 50 have significant DHFR inhibitory activity and are likely to be useful as drugs or after further refinement in the discovery of novel anti-staphylococcal agents.

## ACKNOWLEDGMENTS

The authors are grateful to the authorities of Sree Vidyanikethan College of Pharmacy, Tirupati for the facilities.

## REFERENCES

- Mandell GL, Moorman DR. Treatment of experimental staphylococcal infections: Effect of rifampin alone and in combination on development of rifampin resistance. *Antimicrob Agents Chemother* 1980;17:658-62.
- Tissot-Dupont H, Gouriet F, Oliver L, Jamme M, Casalta JP, Jimeno MT, *et al.* High-dose trimethoprim-sulfamethoxazole and clindamycin for *Staphylococcus aureus* endocarditis. *Int J Antimicrob Agents* 2019;54:143-8.
- Paul M, Bishara J, Yahav D, Goldberg E, Neuberger A, Ghanem-Zoubi N, *et al.* Trimethoprim-sulfamethoxazole versus vancomycin for severe infections caused by methicillin resistant *Staphylococcus aureus*: Randomised controlled trial. *BMJ* 2015;350:h2219.
- Chiacchio MA, Iannazzo D, Romeo R, Giofrè SV, Legnani L. Pyridine and pyrimidine derivatives as privileged scaffolds in biologically active agents. *Curr Med Chem* 2019;26:7166-95.
- Wahlberg G, Adamson U, Svensson J. Pyridine nucleotides in glucose metabolism and diabetes: A review. *Diabetes Metab Res Rev* 2000;16:33-42.
- Prachayasittikul S, Pingaew R, Worachartcheewan A, Sinthupoom N, Prachayasittikul V, Ruchirawat S, *et al.* Roles of pyridine and pyrimidine derivatives as privileged scaffolds in anticancer agents. *Mini Rev Med Chem* 2017;17:869-901.
- Jain AK, Vaidya A, Ravichandran V, Kashaw SK, Agrawal RK. Recent developments and biological activities of thiazolidinone derivatives: A review. *Bioorg Med Chem* 2012;20:3378-95.
- Kerru N, Gummidi L, Bhaskaruni SV, Maddila SN, Jonnalagadda SB. Ultrasound-assisted synthesis and antibacterial activity of novel 1, 3, 4-thiadiazole-1 H-pyrazol-4-yl-thiazolidin-4-one derivatives. *Monatshefte Für Chemie Chem Mon* 2020;151:981-90.
- Patel NB, Soni HI, Parmar RB. Significance of microwave irradiation in synthesis of thiazolidin-4-one bearing pyrimidine analogues: Their *in vitro* antimicrobial, antituberculosis and antimalarial studies. *Curr Microw Chem* 2020;7:230-7.
- Mandal MK, Ghosh S, Naesens L, Bhat HR, Singh UP. Facile synthesis, antimicrobial and antiviral evaluation of novel substituted phenyl 1, 3-thiazolidin-4-one sulfonyl derivatives. *Bioorg Chem* 2021;114:105153.
- Saini N, Sharma A, Thakur VK, Makatsoris C, Dandia A, Bhagat M, *et al.* Microwave assisted green synthesis of thiazolidin-4-one derivatives: A perspective on potent antiviral and antimicrobial activities. *Curr Res Green Sustain Chem* 2020;3:100021.
- Ghoneim AA, Zordok WA. An efficient procedure of synthesis, DFT calculation and theoretical investigation of 4-thiazolidinone fused thiopyrimidine derivatives as antimicrobial agents. *Polycycl Aromat Compd* 2021;42:1-6.
- Srikala R, Mohanalakshmi S. Molecular docking and *in silico* pharmacokinetic parameters of substituted thiazolidin-4-ones as anti-tubercular agents. *Ann Rom Soc Cell Biol* 2021;4:6443-51.
- Heaslet H, Harris M, Fahnoe K, Sarver R, Putz H, Chang J, *et al.* Structural comparison of chromosomal and exogenous dihydrofolate reductase from *Staphylococcus aureus* in complex with the potent inhibitor trimethoprim.



- Proteins 2009;76:706-17.
15. Reeve SM, Scocchera E, Ferreira JJ, G-Dayanandan N, Keshipeddy S, Wright DL, *et al.* Charged propargyl-linked antifolates reveal mechanisms of antifolate resistance and inhibit trimethoprim-resistant MRSA strains possessing clinically relevant mutations. *J Med Chem* 2016;59:6493-500.
  16. Sanner MF. Python: A programming language for software integration and development. *J Mol Graph Model* 1999;17:57-61.
  17. O'Boyle NM, Banck M, James CA, Morley C, Vandermeersch T, Hutchison GR. Open babel: An open chemical toolbox. *J Cheminform* 2011;3:33.
  18. Daina A, Michielin O, Zoete V. SwissADME: A free web tool to evaluate pharmacokinetics, drug-likeness and medicinal chemistry friendliness of small molecules. *Sci Rep* 2017;7:1-3.
  19. Daina A, Michielin O, Zoete V. iLOGP: A simple, robust, and efficient description of n-octanol/water partition coefficient for drug design using the GB/SA approach. *J Chem Inform Model* 2014;54:3284-301.
  20. Daina A, Zoete V. A boiled-egg to predict gastrointestinal absorption and brain penetration of small molecules. *ChemMedChem* 2016;11:1117.

**Source of Support:** Nil. **Conflicts of Interest:** None declared.